Estimating Uncertainty in Daily Weather Interpolations: a Bayesian Framework for Developing Climate Surfaces

Adam M. Wilson

Department of Ecology and Evolutionary Biology
University of Connecticut, Storrs, CT

Current Address:
Department of Ecology and Evolutionary Biology
165 Prospect St.
Yale University
New Haven, CT 06520
Telephone: +1 (203)-432-7540
Fax: +1 (203) 432-5176
Email: adam.wilson@yale.edu

John A. Silander, Jr.

Department of Ecology and Evolutionary Biology
University of Connecticut, Storrs, CT

October 2, 2013

Short Title: Uncertainty in Daily Weather Interpolations

Abstract

Conservation of biodiversity demands comprehension of evolutionary and ecological patterns and processes that occur over vast spatial and temporal scales. A central goal of ecology is to understand the climatic factors that control ecological processes and this has become even more important in the face of climate change. Especially at global scales, there can be enormous uncertainty in underlying environmental data used to explain ecological processes, but that uncertainty is rarely quantified or incorporated into ecological models. In this study a climate-aided Bayesian kriging approach is used to interpolate 20 years of daily meteorological observations (maximum and minimum temperature and precipitation) to a 1 arc-minute grid for the Cape Floristic Region of South Africa. Independent validation data revealed overall predictive performance of the interpolation to have R^2 values of 0.90, 0.85, and 0.59 for maximum temperature, minimum temperature, and precipitation, respectively. A suite of ecologically-relevant climate metrics that include the uncertainty introduced by the interpolation were then generated. By providing the high resolution climate metric surfaces and uncertainties, this work facilitates richer and more robust predictive modeling in ecology and biogeography. These data can be incorporated into ecological models to propagate the uncertainties through to the final predictions.

Keywords: interpolation, bayesian, krige, climate metric, ecology

Acknowledgments: This work was supported by NSF grants OISE-0623341, DEB-0516320, and DEB-1046328 to JAS and by NASA headquarters under the NASA Earth and Space Science Fellowship Program grant NNX09AN82H to AMW. We also thank Chris Lennard and Lisa Coop at the Climate System Analysis Group at the University of Cape Town for providing the station data.

1 Introduction

The role of climate in driving ecological processes has been known for 170^+ years (*e.g.* Meyen, 1846). Recently, in the face of climate change, the scientific community has focused its attention on the role of climate and weather in ecological processes, evident in the thousands of publications on the topic since the year 2000. A limiting factor for many ecological studies is the availability of accurate weather and climate data for locations of interest (Hijmans et al., 2005). Unfortunately for this purpose, weather stations are often irregularly spaced and clustered in heavily populated, low elevation areas which may be far from where ecological observations are made or needed. Thus ecologists are faced with the problem of estimating weather/climate for the locations of interest. For many types of analysis, gridded weather/climate data are preferable to point observations because of their spatial continuity (Haylock et al., 2008) and several methods exist for interpolating from station observations to a continuous surface across the region including: nearest neighbor (Stahl et al., 2006), Cressman Interpolation (Cressman, 1959), thin-plate splines (Tait et al., 2006), generalized additive models (Guan et al., 2009), and kriging (Haylock et al., 2008). See Apaydin et al., 2004 for a review of other methods.

This study was motivated by two concerns:

- Ecologists often use output from meteorological and climatological analysis as input for their models without incorporating the uncertainty inherent in the climate product.

- Most climate data used in ecological models are coarse temporal aggregations such as monthly means rather than variables that are known to be more relevant to the ecological process under study, such as the longest period between rain events or absolute minimum temperature.

1.1 Estimating Uncertainty

Scientists are under increasing pressure to improve estimates of uncertainty in both ecology (*e.g.* Cressie et al., 2009) and climate change research (*e.g.* Collins et al., 2006a). Ecologists often use climatological and meteorological model output as input to their analysis as if they were 'truth' despite evidence that the results can vary widely depending on which data are used (Peterson and Nakazawa, 2008; Roubicek et al., 2010; Soria-Auza et al., 2010; Wiens et al., 2009). For example, it is not uncommon to build species distribution models that treat interpolated climate surfaces as data and ignore any uncertainty inherent in the surfaces (*e.g.* Pearson et al., 2007; Raes et al., 2009; Ward, 2007; Williams et al., 2009). Furthermore, producers of climate data often share only the 'best estimates' of the quantities of interest (Daly, 2006) making incorporation of the uncertainty impossible. Perhaps the most commonly cited ($> 2,000$ citations as of July 2013) example of this is the WorldClim data set which offers 30 arc-second (∼1km) resolution globally whether the pixel contains a weather station or the nearest station is hundreds of kilometers away (Hijmans et al., 2005). The value of an interpolated 1km pixel that is hundreds of kilometers from the nearest weather station (a common situation throughout the tropics) is much less certain than that of a pixel located at a weather station, but without any reported uncertainty, one is led to the biased conclusion that the spatial accuracy of the product is uniform. Furthermore, the increased availability of very fine climate surfaces can lead the user to "equate resolution with realism" despite the importance of fine-scale climatological process that are not represented in the interpolation algorithm (Daly, 2006). As ecological models become more complex, it is vital to account for uncertainty inherent in data and propagate it through to the results (Clark and Gelfand, 2006; Luo et al., 2011).

1.2 Climate Metrics

There is growing awareness that organisms may respond more to climate extremes and other climate metrics (such as annual minimum temperature, growing season length, and the longest annual period between precipitation events) than mean values (Gutschick and BassiriRad, 2003; Jackson et al., 2009; Trnka et al., 2011). However these more proximal metrics are more difficult to calculate because they generally require daily (or more frequent) meteorological observations. The use of coarse aggregate metrics, such as monthly means, is typically supported with the argument that they tend to be correlated with more proximal variables across space (Jackson et al., 2009). However, when the goal is prediction of ecological processes, such as phenology (e.g. Richardson et al., 2006), demographics (e.g. Clark, 2003; Colchero et al., 2009), or disturbance (e.g. Wilson et al., 2010) into new areas or times, models that capture more direct mechanistic relationships are likely to have better predictive performance (Jackson et al., 2009). Furthermore, global change may lead to a temporal decoupling between the aggregate measures and the more proximal variables that directly affect the ecological process of interest (Jackson et al., 2009).

As many of these metrics are sensitive to daily meteorological events, ignoring the uncertainty in each day's predictions makes it impossible to estimate uncertainty in the metrics or in any subsequent analysis. For example, the longest annual dry spell could be cut in half by a single rain event. Methods that result in a single-valued prediction for rainfall on a given day will result in a single estimate of the longest annual dry spell with no accounting for the uncertainty in each day's rainfall prediction, regardless of the distance to the nearest station. It is thus difficult, if not impossible, to estimate uncertainty in these metrics using traditional interpolation methods that result in only 'best estimates' of daily weather.

1.3 Bayesian Solution

Bayesian methods are capable of generating a full posterior distribution of all unknown model parameters (Clark, 2004) and are becoming more common in climatological analyses (e.g. Fischer et al., 2012; Iizumi et al., 2012; Ruggieri, 2013). Thus a Bayesian interpolation results in a distribution of meteorological values for each prediction location for each time. It is possible to sample from these distributions of daily meteorology and generate any climate metric of interest. For example, we can draw 1,000 precipitation values from each day's posterior distribution for a given year and calculate 1,000 realizations of length of the longest dry spell. From this distribution, any summary of interest (such as the mean or variance) can be derived with credible intervals.

In this study a framework is presented to interpolate daily station weather data (maximum and minimum temperature and precipitation) to high resolution surfaces, calculate relevant climate metrics (see Kimball et al., 2012, for a discussion of selecting relevant metrics for plants), and keep track of the uncertainties introduced by the interpolation. For simplicity, in this paper the interpolated surfaces of daily weather data are referred to as 'meteorological' surfaces and the derivative metrics (such as growing degree days) as yearly 'climate metrics,' even though they are not long-term (multi-decadal) aggregations. The yearly 'climate metrics' could be further processed to produce typical climatologies that summarize the parameter over many years (*e.g.* the 30-year distributions of annual growing degree days). While other studies have used Bayesian methods to interpolate meteorological surfaces (Alvarez-Villa et al., 2011; Cooley et al., 2007; Fasbender and Ouarda, 2010; Johansson and Glass, 2008; Newlands et al., 2011; Riccio, 2005; Sang and Gelfand, 2009), to our knowledge this is the first effort to use the posterior distributions to generate surfaces of ecologically-relevant climate metrics that incorporate the uncertainty introduced by the interpolation process.

2 Methods

2.1 Study Area

The Cape Floristic Region (CFR) of South Africa (~90,000 km^2) is home to almost 9,000 species, 65% of which are endemic (Goldblatt, 1997). Species in the CFR tend to be locally abundant but have small ranges and limited dispersal capabilities (Latimer et al., 2005). These factors suggest that the region's biodiversity may be sensitive to shifts in the precipitation regime predicted under future climate change (Christensen et al., 2007, section 11.2.3). The region is topographically and climatically diverse, with elevations ranging from sea level to over 2,000m and mean annual rainfall ranging from 60mm to greater than 3,300mm (Schulze, 2007). In this study, we interpolate 20 years (1990-2010) of daily weather (maximum temperature, minimum temperature, and precipitation) observations to a 1 minute (~1.55km x 1.85km) grid for the CFR.

2.2 Modeling

Large, topographically heterogeneous regions present challenges for interpolation of weather, especially precipitation. Several recent studies have revealed that interpolating anomalies of daily weather from long-term or monthly means rather than the raw, observed values can lead to improved prediction accuracy (*e.g.* Haylock et al., 2008; Hunter and Meentemeyer, 2005). The framework described in these studies was used to calculate the daily anomolies for each station from long-term climate surfaces as follows for precipitation:

$$P_{\text{anomaly}} = \frac{P_{\text{daily}}}{P_{\text{monthly}}} \tag{1}$$

and temperature:

$$T_{\text{anomaly}} = T_{\text{monthly}} - T_{\text{daily}} \tag{2}$$

Classical geostatistical inference (Kriging) treats interpolation as two separate steps, parameter estimation and prediction (Diggle and Ribeiro, 2007). In common practice, the best estimate of the interpolation parameters is "plugged in" as if it were truth and the uncertainty in the model parameters is not propagated through to the prediction variance. This procedure often leads to an overestimate of the certainty of the predictions. To overcome this limitation, we applied the 'bayesian krige' described by Diggle and Ribeiro (2007, Section 7.2.3). This approach treats the kriging parameters: the sill (σ^2) , range (ϕ), and nugget (τ) as random variables and thus the predictive distribution incorporates their uncertainty (Figure 1). In addition, like co-kriging, the model also allows additional co-variates ($\mathbf{X}$) to be included in a regression framework. Because the response data are daily anomalies from the mean (rather than the absolute daily values), there is little fine-grain variability corresponding to local environmental conditions (such as elevation). In other words, a day that is colder than average tends to be colder than average both at the top and the bottom of a mountain. In this study we include both latitude and longitude to allow linear trends in both dimensions. The coefficients for these variables are represented by $\boldsymbol{\beta}$. The model can be written as follows, where ($\mathbf{u}$) represents locations (from Ribeiro Jr and Diggle, 2009, Section 4.5):

$$\mathbf{Y}(\mathbf{u}) = \mathbf{X}\boldsymbol{\beta} + \sigma T(\mathbf{u}) + \varepsilon(\mathbf{u}) \tag{3}$$

$$T(\mathbf{u}) \sim \mathcal{N}(0, R(\phi)) \quad \text{and} \quad \varepsilon \overset{\text{i.i.d}}{\sim} \mathcal{N}(0, \tau^2) \tag{4}$$

consequently,

$$pr(Y|\boldsymbol{\beta}, \sigma^2, \phi, \tau_R^2) \sim \mathcal{N}\big(X\boldsymbol{\beta}, \sigma^2 R(\phi, \tau_R^2)\big) \tag{5}$$

where

$$R(\phi, \tau_R^2) = \sigma^2\big[R(\phi) + \tau_R^2 \mathcal{I}\big] = \sigma^2\Big[R(\phi) + \frac{\tau^2}{\sigma^2}\mathcal{I}\Big]. \tag{6}$$

We used the `krige.bayes` function in the `geoR` package (Diggle and Ribeiro Jr, 2001) of R ({R Development Core Team}, 2011, v2.12.1) to perform the day-by-day interpolations. This function simplifies model fitting with discretized prior distributions for ϕ and the 'noise to signal variance ratio' ($\tau_R^2 = \frac{\tau^2}{\sigma^2}$). A discretized reciprocal prior was used for σ^2 and $\frac{\tau^2}{\sigma^2}$ and a discretized exponential prior was used for ϕ (see Diggle and Ribeiro Jr, 2002, for a discussion of various choices for these parameters).

The prediction of the daily anomalies was done on a $^1/_4$ degree grid which was then down-sampled to the 1-minute climate grid using a bi-cubic resampling algorithm. Computational limitations prevented making the predictions at the full one minute resolution (see Section 2.6). However, as anomaly surfaces are "relatively free of the considerable topography-forced spatial variability," (Willmott and Robeson, 1995) the surfaces at $^1/_4$ degree are relatively smooth. The high resolution anomaly surfaces were then converted back to the original units (^{o}C for temperature and mm for precipitation) by inverting the relationships in Equations 1 and 2.

2.3 Data

Daily weather observations were collected from $\sim$700 weather stations (70 temperature and 645 precipitation) across the region (Figure 2) by the South African Weather Service (SAWS, `http://www.weathersa.co.za/`) and the South African Computing Center for Water Research (University of Natal, P/Bag X01, Scottsville 3209, South Africa). These data were assembled and quality controlled by the Climate Systems Analysis Group at the University of Cape Town (CSAG, `http://www.csag.uct.ac.za/`) based on measures used by the daily Global Historical Climate Network (Williams et al., 2006). We used long-term monthly climate surfaces of mean monthly maximum and minimum temperature and total precipitation. These surfaces were developed from quality controlled station observations from the period for 1950-2000 as described in Schulze (2007). These high resolution climate surfaces facili-

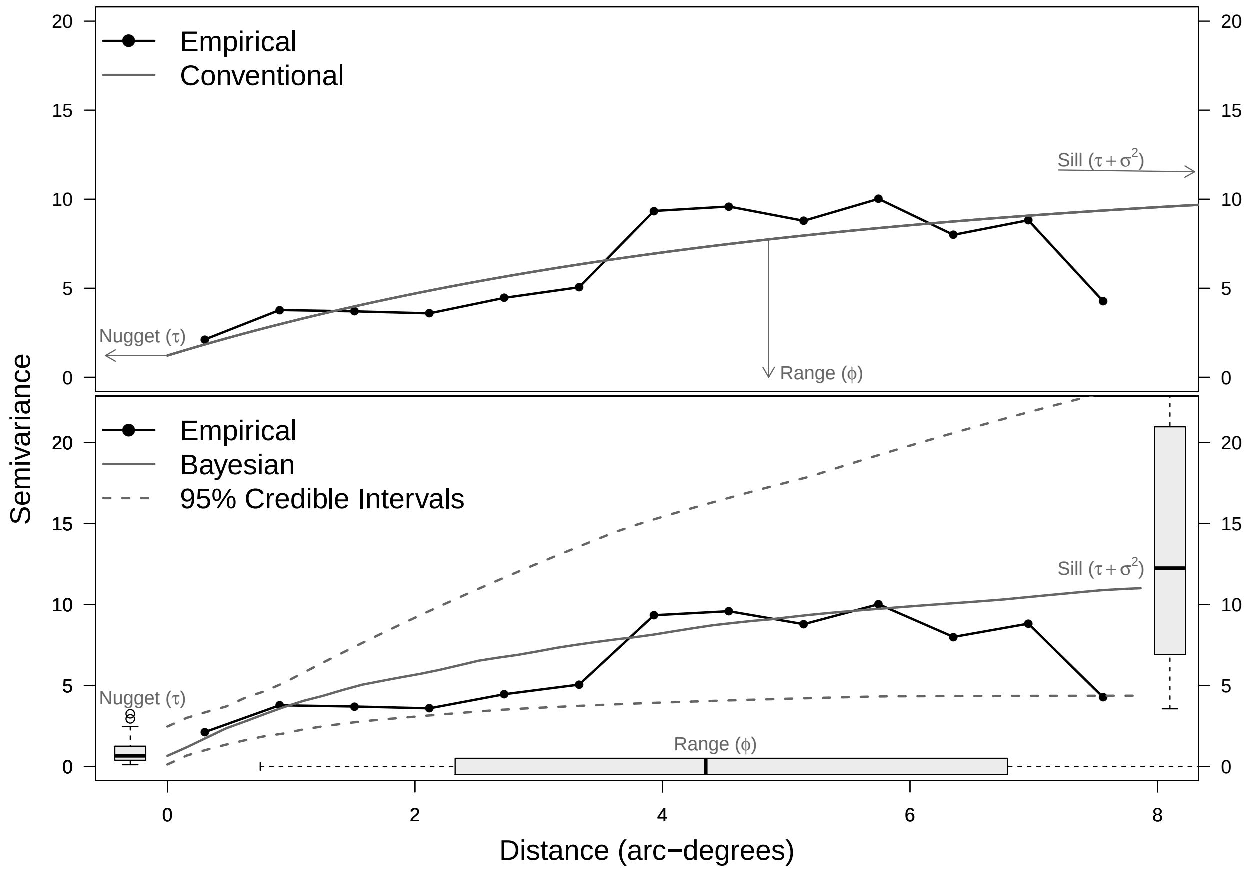

Figure 1: Empirical (black) and fitted (grey) semivariograms for maximum temperature on January 3, 2009. The top panel shows the variogram and spatial parameters fitted using conventional techniques, while the bottom panel shows the Bayesian variogram with 95% credible intervals. The box plots on the X and Y axis represent the posterior distributions of the three spatial parameters: the sill (σ^2) , range (ϕ), and nugget (τ). Note that the median Bayesian curve is very similar to the conventional variogram, but the Bayesian method quantifies the uncertainty in the variogram due to uncertainty in the kriging parameters.

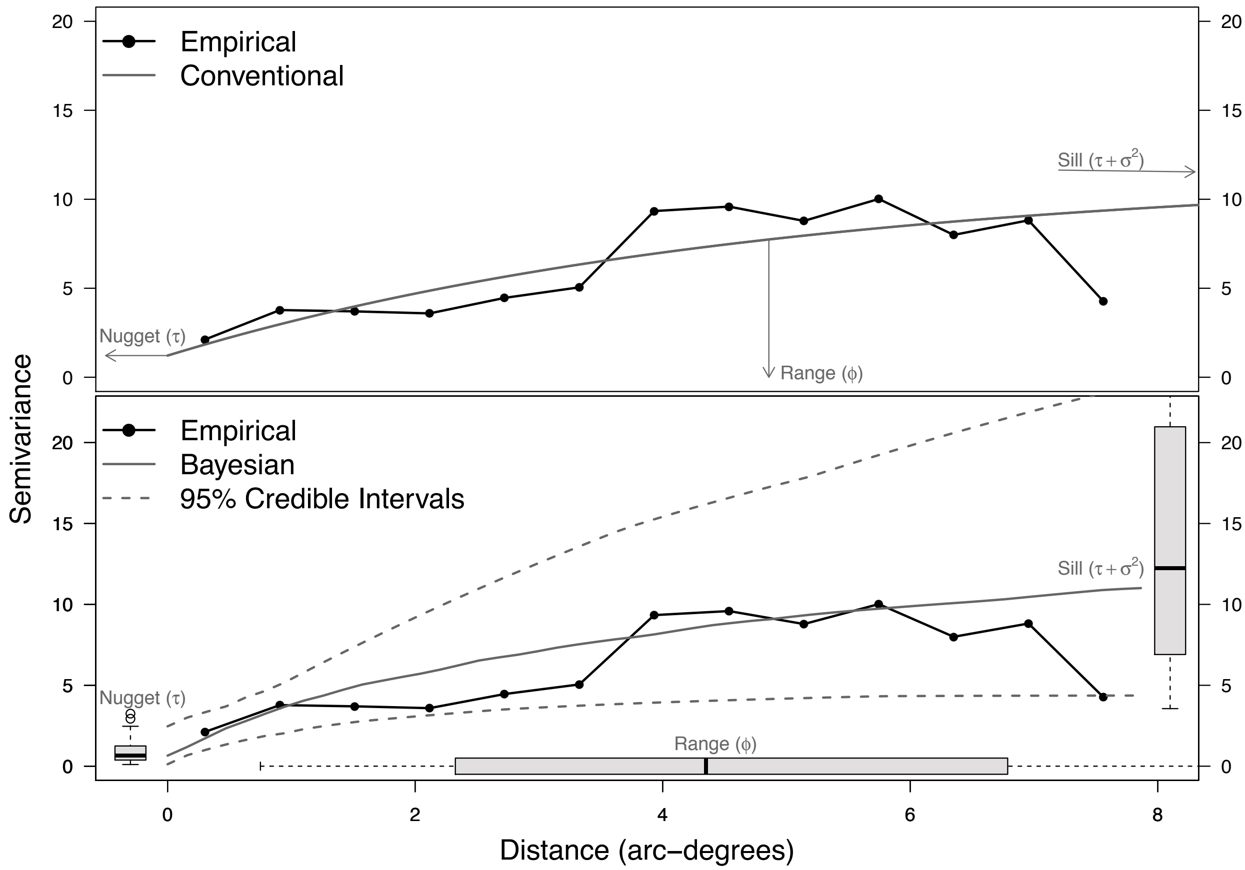

Figure 1: Empirical (black) and fitted (grey) semivariograms for maximum temperature on January 3, 2009. The top panel shows the variogram and spatial parameters fitted using conventional techniques, while the bottom panel shows the Bayesian variogram with 95% credible intervals. The box plots on the X and Y axis represent the posterior distributions of the three spatial parameters: the sill (σ^2) , range (ϕ), and nugget (τ). Note that the median Bayesian curve is very similar to the conventional variogram, but the Bayesian method quantifies the uncertainty in the variogram due to uncertainty in the kriging parameters.

tated incorporation of spatial and temporally varying lapse rates that are based on >50-year time series and other sources of information (see Schulze, 2007, for details).

2.4 Climate Metrics

A set of climate metrics was selected to target various aspects of plant performance in the CFR (Table 1). For example, seedling survival in the region is sensitive to summer drought (Midgley, 1988), which was quantified by the length of the longest dry spell, and germination of some species may require stratification by sufficiently cold minimum temperatures (Keeley and Bond, 1997), which is quantified with the absolute minimum temperature of the year. The other biologically relevant metrics are summarized in Table 1. The climate metrics were calculated for each location using a time series consisting of samples from each day's posterior distribution for each year. This process resulted in a posterior distribution for each climate metric, for each pixel, for each year. These distributions were then summarized to derive the mean, standard deviation and credible intervals of the predicted metrics.

2.5 Validation

The models were evaluated in two ways. During model fitting, observations from three randomly selected stations were held out each day. Three stations were selected to ensure some spatial coverage for each day without impacting the performance of the model. This sub-setting resulted in over 20,000 validation observations that were not used in model fitting. The mean posterior predictions for these locations were then compared with the observed data to assess the predictive accuracy using the coefficient of determination, root mean square error, mean absolute error, and mean error. In addition, for precipitation, the model's ability to predict 'wet days' where $ppt \geq 2mm$ was assessed using the positive predicted value (% predicted wet that were wet) and negative predicted value (% predicted

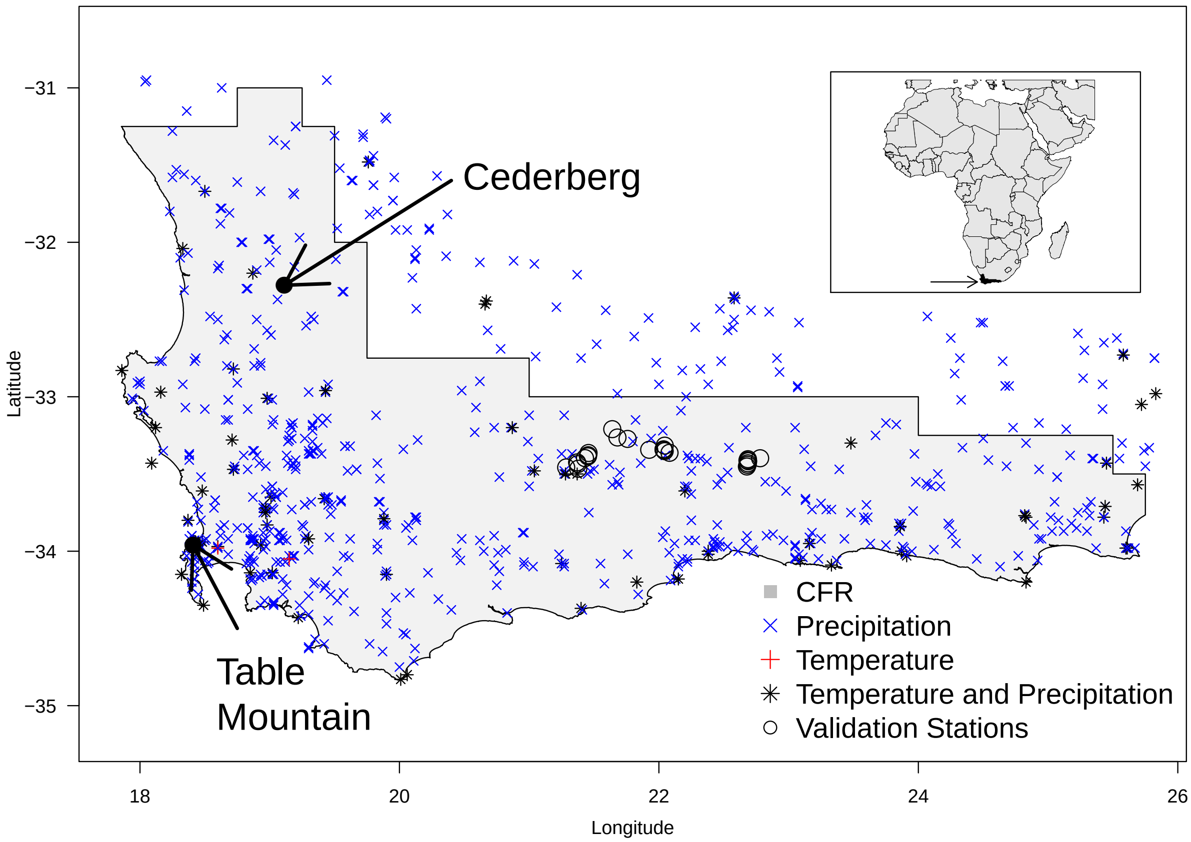

Figure 2: Map of the Cape Floristic Region (CFR, in gray) of South Africa showing locations of various types of weather stations included in this study. Stations within 75km of the CFR were included to aid in interpolation near the edges of the region. The validation stations are locations with monthly data that were not included in the interpolation. Filled circles show locations of the two example locations discussed in the text. Inset shows location of the CFR within Africa.

dry that were dry).

The second evaluation was to calculate monthly maximum and minimum temperature and monthly total precipitation for additional locations in the study area where monthly total precipitation and monthly minimum and maximum temperature are available (Figure 2). These stations, maintained by the CapeNature Management organization (`http://www.capenature.co.za/`) are all in mountainous areas and represent the most difficult prediction locations and are thus useful for evaluating the product for use in these remote regions. This validation is also useful to assess any temporal bias resulting from modeling each day independently.

2.6 Computational Notes

Fitting the daily models in this framework is computationally demanding in terms of both storage and processing. The models were run on a cluster of 74 Xeon E5530 2.4GHz quad-core hyper-threading CPUs at the University of California Davis (making >500 threads available for processing). Processing the 20 years of data required ≈200 processor days to complete. The posterior samples for each day were converted to netCDF v4.0 format and summarized with the NCAR Climate Language ({National Center for Atmospheric Research}, 2011), the NetCDF Climate Operators (Zender, 2008), and the Climate Data Operators (Mueller and Schulzweida, 2013) using R ({R Development Core Team}, 2011) as the overall scripting language. The full posterior dataset (consisting of 1000 iterations of maximum and minimum temperature and precipitation at 1 minute resolution for each day) requires over 7 terabytes of disk space.

Quantity	Description	Plant performance elements	Input Data	Functional form
MinT	Annual minimum temperature	Seed stratification, germination, growth	t_{min}	$\min(t_{min})$
MaxT	Annual maximum temperature	Germination, growth, Seedling mortality	t_{max}	$\max(t_{max})$
FD	Frost days	Seedling mortality	t_{min}	$\sum_{t \in \text{year}}(t_{min_t} < 0^oC)$
CFD	Longest consecutive period with frost	Seedling mortality	t_{min}	max(consecutive($t_{min} < 0^oC$))
GDD	Growing Degree Days	Growth	t_{max}	$\sum_{t \in \text{year}} \max(t_{min_t} - 10.0)$
CSU	Consecutive Summer Days ($> 35^oC$)	Seedling mortality	t_{max}	max(consecutive($t_{max} > 35^oC$))
CDD	Annual maximum consecutive dry days	Growth, Seedling mortality	*ppt*	max(consecutive(*ppt* <2mm))
ECA	Very heavy precipitation days	Growth, Seedling mortality	*ppt*	Number of days with *ppt* >20mm
SDII	Simple daily precipitation intensity index	Growth, Seedling mortality	*ppt*	mean(*ppt*) where *ppt* >2mm

Table 1: Climate metrics were calculated using 1,000 time series drawn from the posterior samples in each location to result in a posterior distribution that incorporates the uncertainty introduced by the interpolation. Climate metrics were calculated using CDO tools (Mueller and Schulzweida, 2013).

3 Results

3.1 Validation of Daily Data

Overall, the model achieved high predictive accuracies for daily minimum and maximum temperature ($R^2 = 0.85$ and $R^2 = 0.90$, respectively), and moderate accuracy for precipitation ($R^2 = 0.59$) (Figures 3, 4, and Table 2). The mean absolute errors were generally low for all variables (1.26^oC for both maximum and minimum temperature, and 0.85mm for precipitation). The model successfully predicted dry days ($\leq 2mm$) 97% of the time and wet days 66% of the time. Figure 4 shows the predicted vs. observed scatterplots grouped by month. The predictive accuracy is relatively similar throughout the year.

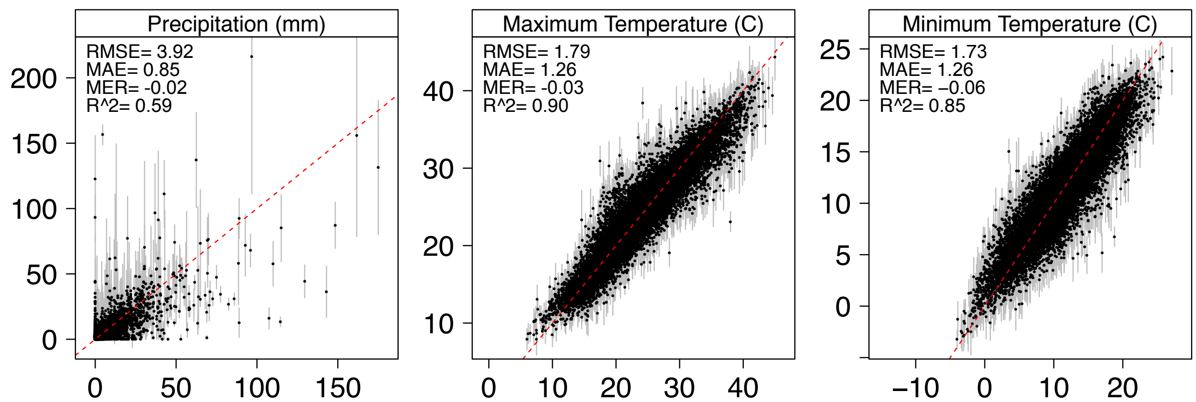

Figure 3: Scatterplot of predicted and observed weather from the three hold-out validation observations from each day during 1990–2009 (totaling ≈20,000 observations). The units for both x and y axis are ^{o}C for temperature and mm for precipitation. Grey bars represent ± 1 standard deviation of the posterior distributions. The dashed lines indicate $y = x$. The validation metrics are as follows; RMSE: Root Mean Squared Errors, MAE: Mean Absolute Error, MER: Mean Error

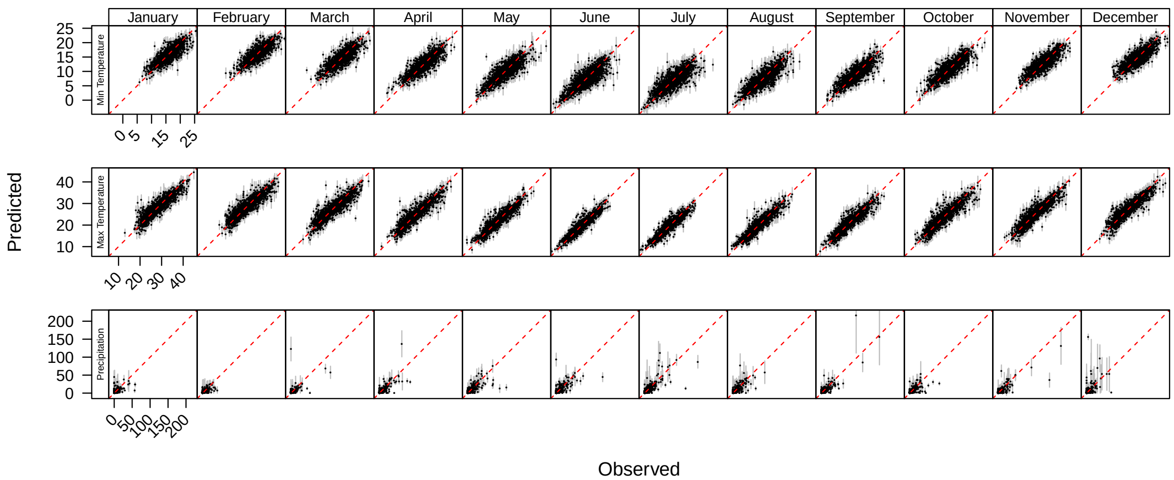

Figure 4: Scatterplot of predicted and observed weather from the daily hold-out validation stations separated by month (columns). The units for both x and y axis are ^{o}C for temperature and mm for precipitation. Grey bars represent ± 1 standard deviation of the posterior distributions. The dashed lines indicate $y = x$.

	Daily data					Monthly data				
Variable	RMSE	MAE	MER	R^2	n	RMSE	MAE	MER	R^2	n
Maximum Temperature (^{o}C)	1.79	1.26	-0.03	0.90	21,915	4.93	3.79	0.67	0.60	1,280
Minimum Temperature (^{o}C)	1.73	1.26	-0.06	0.85	21,915	3.39	2.67	1.02	0.48	1,138
Precipitation (mm)	3.92	0.85	-0.02	0.59	21,915	29.61	19.71	-3.60	0.56	5,036

Table 2: Validation results for each variable. The comparison of daily data are from the daily observations not included in model fitting. The monthly data compare predicted and observed total monthly precipitation and monthly maximum and minimum temperature at a set of remote stations. The poorer fit for the monthly temperature is expected as it represents the ability of the model to estimate the single daily maximum and minimum in each month, while the monthly precipitation comparison is the aggregated total for the month. The validation metrics are as follows. RMSE: Root Mean Squared Errors, MAE: Mean Absolute Error, MER: Mean Error

3.2 Validation of Monthly Data

The validation of the monthly data resulted in lower predictive accuracy than the validation of the daily data for maximum and minimum temperature ($R^2 = 0.60$ and $R^2 = 0.48$, respectively), but a similar value for precipitation ($R^2 = 0.56$, Table 2). The lower correlations for temperature are expected because the weather stations recorded the absolute minimum and maximum temperature (rather than the monthly mean of the daily extremes) and are thus sensitive to a single day's value. The precipitation data, on the other hand, represent the monthly sum and so the comparison is less sensitive to each day's value.

3.3 Spatial and temporal variability of uncertainty

This interpolation method results in full posterior distributions for daily minimum temperature, daily maximum temperature, and precipitation. These distributions can be used to derive any quantities of interest from the daily weather values to any derived climate metric. For example, Figure 5 shows the posterior mean and coefficient of variation (CV, $\frac{\sigma}{\mu}$) of the longest period of consecutive dry days (CDD) across the region for the year 2000. CDD is a critical climate metric affecting plant survival and reproduction and hence distribution in some ecosystems (Kimball et al., 2012). In this plot, the contours reveal the complex topography of uncertainty in the posterior distributions of cumulative dry days. Note the complex 'ridges' of uncertainty that exist between stations. The inset plot shows the relationship between the mean and CV. The arc-like structures are a function of distance to the nearest station. The mean and CV of four climate metrics representing extremes in both temperature and precipitation for the year 2000 are shown in Figure 6. The longest period of consecutive dry days (CDD) tends to be higher in the north-eastern mountains and arid interior and lower in southern coastal regions while the CV tends to have depressions in locations near stations. The longest period of consecutive frost days (CFD) is higher in interior mountains and lower in coastal areas in contrast to the CV of CFD, which tends to be low in the mountains and higher in the coastal areas. The lower elevations in the northwest portion of the region has more consecutive summer days (CSU) than the southeast. The number of large precipitation events (ECA) is highest in the southeastern mountains and eastern coastal areas, and lowest in the arid interior. The posterior distributions of the predictions for climate metrics in each year at both of the example locations shown in Figure 2 are illustrated in Figure 7. The within-year variability represents uncertainty about what the 'true' value was for that location in that year. In Figure 7 it is clear that there are significant year-to-year differences across the various metrics. Some years (*e.g.* 1999) are warm and dry at both sites while some years (*e.g.* 1996) are cooler and wetter. As several of the metrics are sensitive to the events on a single day (such as CDD and CFD), there can be considerably more uncertainty in the estimated value and that uncertainty can vary from year to year. For example, the mean estimated CDD for the Cederberg location in 1994 (69 days) was similar to 1997 (66 days), but the inter-quartile widths (IQW; 2.5%–95%) were 10 and 33 days, respectively (Figure 7). In contrast, the mean estimates for the Table Mountain location in 1994 and 1997 were both 17 days, while the IQW's were 16 and 10 days, respectively. The differences in the variance of the predictions for the two locations are primarily due to Table Mountain's location in an area with ten stations within 3km, while the Cederberg site's closest station is more than 10km away. These metrics are much more sensitive than long-term or even monthly means to infrequent extreme climate events that are critical to explaining the occurrence and distribution of species across a region.

4 Discussion

The uncertainties in the climate metrics reflect sparseness in weather station data along with complexity in landscape topography and the metrics themselves. If meteorological observations were available for every square kilometer across the region, there would be little spatial variability in the uncertainty in any interpolation at a comparable resolution. Likewise, if the topography were flat and the weather driven primarily by large frontal systems, an equivalently sparse weather station network would yield lower uncertainty than in topographically-heterogeneous landscapes. The results illustrate the value of quantifying the uncertainty of interpolated weather surfaces across space and time. It is possible that changes to the modeling structure (such as altering the spatial decay function) or priors could improve the predictive performance of this model for this set of data, but predictive uncertainties will always be present in any interpolated surface. Our intention here was to demonstrate an interpolation method capable of propagating interpolation uncertainties through to the final estimates of ecologically relevant climate metrics.

The maps in Figure 6 illustrate that even in a region of the world with a relatively high density of reliable weather stations, there is still considerable uncertainty in the interpolated predictions (whether or not the uncertainties are estimated). Furthermore, the spatial uncertainty in the interpolated climate metrics is a complicated function of distance to the nearest station and the properties of the metric itself. For example, note the extreme spatial variability of the CV of CDD in Figure 5. South of 34^oS, the CV surface is relatively

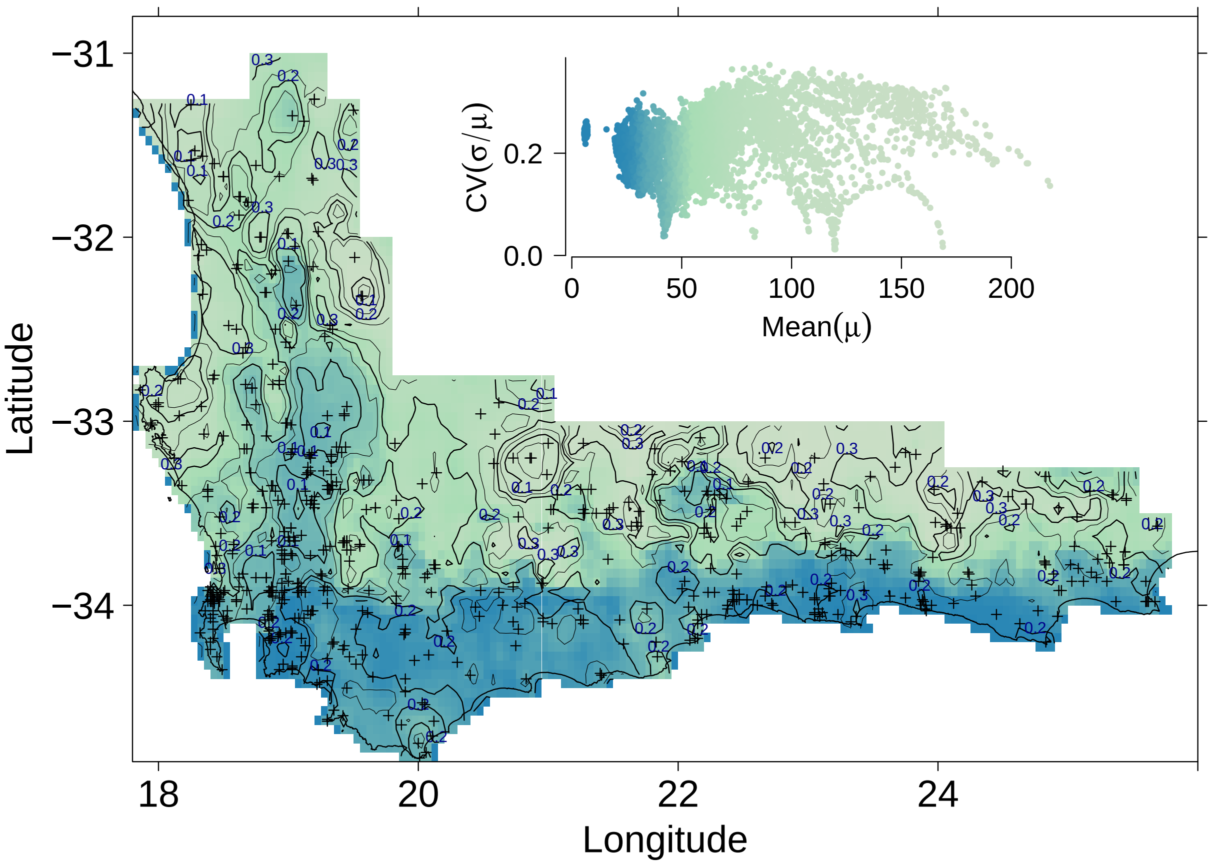

Figure 5: Map illustrating the longest period of cumulative dry (precipitation < 2mm) days for the year 2000. Mean posterior values are shown in shades of grey with the coefficient of variation (CV) of the posterior distributions ($\frac{\sigma}{\mu}$) overlaid as contours. The inset plot shows the relationship between the mean posterior values and the CV and serves as a key for the map. The arcs are a function of distance to the nearest meteorological station, with lower coefficient of variation in pixels close to stations. The white crosses indicate locations of meteorological stations with data used in the interpolation. Note that between stations in drier areas there are often 'ridges' of uncertainty, while in wetter areas the uncertainty is lower due to frequent precipitation events.

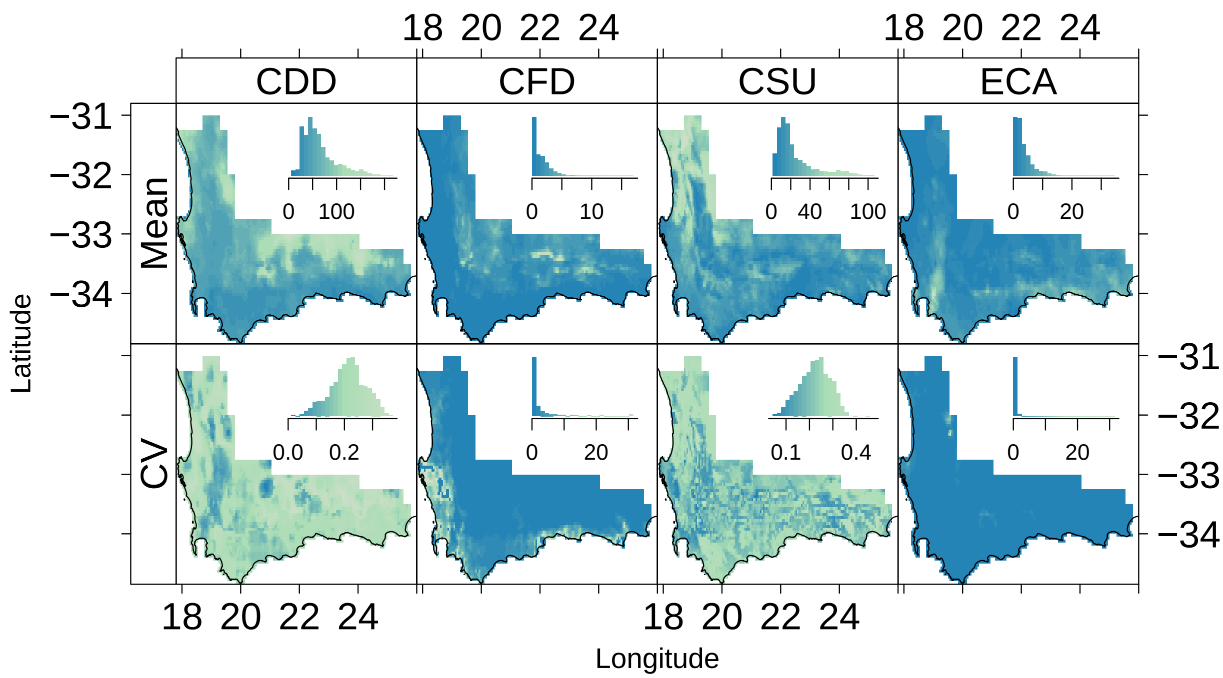

Figure 6: Maps illustrating the mean (top row) and coefficient of variation (bottom row) of the posterior samples for four climate metrics for the year 2000: consecutive dry days (CDD), consecutive frost days (CFD), consecutive summer days (CSU) and the number of rain events > 20mm (ECA). See Table 1 for a description of each metric. The histograms show the distribution of values within each panel. Note that the coefficient of variation of the predictions is a complicated function of distance to the nearest station and the predicted value.

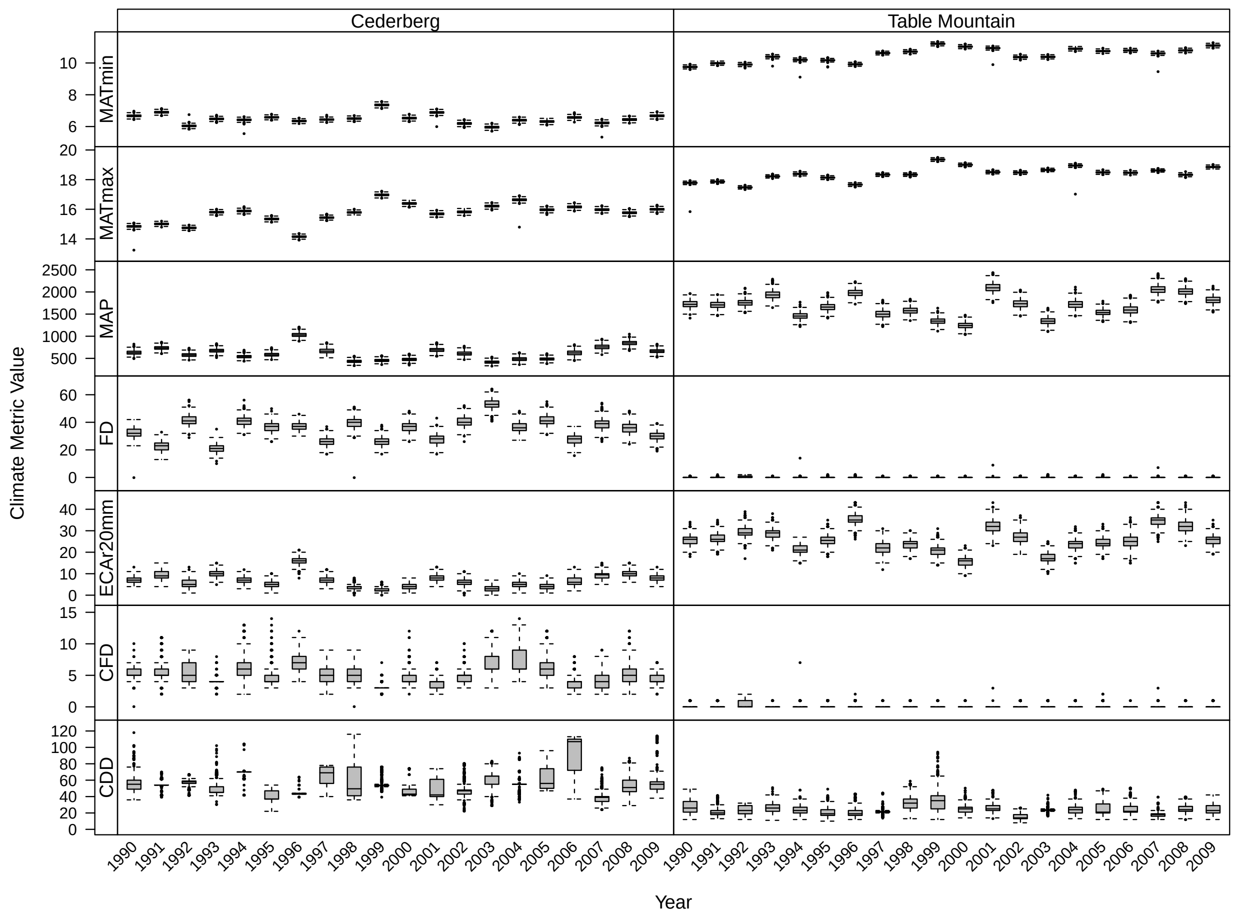

Figure 7: Comparison of the posterior distribution of the climate metrics (see Table 1) for two locations (Cederberg and Table Mountain, see Figure 2). Variables include: mean annual minimum temperature (MATmin, ^oC), mean annual maximum temperature (MATmax, ^oC), mean annual precipitation (MAP, mm), number of frost days (FD), the number of rain events $>$ 20mm (ECAr20mm), consecutive frost days (CFD), and consecutive dry days (CDD). Table Mountain has ten stations within 3km, while the Cederberg's closest station is over 10km away.

smooth while north of 34^oS, the surface is very irregular and highly sensitive to the locations of stations. Because the inland areas are more arid, there is greater potential for a large CDD and thus locations far from stations have large uncertainty in the predicted values. In contrast, southern coastal areas (which receive more regular rainfall) have both lower CDD and associated CV, even in areas far from stations (*e.g.* 21^oE, 34.5^oS).

4.1 Implications of climate data uncertainty in ecological modeling

Ecologists are under increasing pressure to make predictions about ecological change (Clark et al., 2001). Detecting, attributing, and predicting ecological change requires techniques that carefully account for the uncertainty inherent in an increasing variety of data sources including traditional field observations, remote sensing (Muraoka and Koizumi, 2009), embedded sensor networks (Clark et al., 2011; Collins et al., 2006b), and interpolated climate data (Roubicek et al., 2010; Soria-Auza et al., 2010). The intention of this study was to illustrate how a Bayesian framework can propagate the uncertainty in interpolations of daily meteorological data through to the final surfaces of ecologically and biologically relevant climate metrics and provide posterior distributions that can later be incorporated into ecological analysis.

Previous work has revealed that the choice of weather data can make a significant impact on the results of ecological analysis. For example, Soria-Auza, et al. (2010) used the MaxEnt framework (Elith et al., 2011) to compare estimate species distributions using climate data available via WorldClim (Hijmans et al., 2005) and SAGA (Bhner, 2005). Even though the differences these datasets were relatively minor (correlations ranged from 0.46 to 0.99 across climate variables), the authors reported significant differences in the predictions in some regions. In a similar fashion, Peterson and Nakazawa (2008) compared species distribution models for fire ants (*Solenopsis invicta*) developed using climate data from three sources: WorldClim (Hijmans et al., 2005), the Hadley Climate Model (Johns et al., 1997), and the Center for Climate Research at the University of Delaware (Feddema, 2005). They found significant differences in the predicted distributions developed using the various climate data sets. In both of these studies, the authors used additional information to assess the relative merit of the predictions derived from various climate data (WorldClim performed worse in both cases). However, it is common in distribution modeling studies that no independent climate data (or interpolation uncertainties) are available and thus ecologists are faced with either arbitrarily choosing a climate dataset or making predictions with multiple climate datasets and noting the differences.

The situation is similar to the use of output from global climate models (GCMs). Typically the output from multiple GCMs are treated independently in ecological analysis (e.g. Beaumont et al., 2008; Lawler et al., 2009) and the differences are explored by comparing the resulting predictions. Alternatively, sometimes the mean of several GCMs are used (Ahmed et al., 2013). This is analogous to the independent comparisons of different climate interpolations mentioned above. There has been some recent effort to develop probabilistic climate projections by treating output from different GCMs as 'samples' from a 'true' future climate (Tebaldi and Knutti, 2007) which would allow probabilistic ecological projections. This approach has not yet been widely adopted, in part because the uncertainties in the output from GCM ensembles are difficult to quantify due to lack of verification and model dependence, bias, and tuning (Tebaldi and Knutti, 2007). In contrast, the uncertainties inherent in interpolating climate data from station observations are much more tractable and the methodology presented here results in probabilistic spatio-temporal estimates that can be incorporated into further ecological analysis.

For example, recent developments in Bayesian species distribution models are capable of incorporating co-variate data into the model as a random variable and thus account for the uncertainty of the data in the results. See Chakraborty et al. (2010, 2011) and McInerny and Purves (2011) for examples of species distribution models that could incorporate the uncertainty of the climate metrics via Markov chain Monte Carlo sampling. Propagating this uncertainty could be achieved relatively easily by considering the environmental variables to be random variables and sampling from their interpolated posterior distributions in each iteration of model fitting. For example, consider a simple linear regression that could be used to explain ecological performance (such as the growth or reproduction of individuals across space or time) as a function of its environment, $\boldsymbol{y} \sim \mathcal{N}(\boldsymbol{X\beta}, \sigma^2)$ where $\boldsymbol{y}$ is a vector of $i \in 1 : I$ observations of performance in different locations/times and $\boldsymbol{X}$ is a $I \times P$ matrix of P co-variates for each location/time. Typically the matrix of explanatory variables ($\boldsymbol{X}$) is considered to be known exactly even when, as is usually the case, the data have associated uncertainties. By adding another level to the model which samples the $\boldsymbol{X}$'s from a distribution (such as the climate metrics described in this paper), $X_{I\times P} \sim \mathcal{N}(\mu_{I\times P}, \sigma^2_{I\times P}\mathcal{I}_{I\times P})$, the uncertainty in the environmental variables will be propagated through to the predictions of the model. A similar approach has been recently explored in epidemiological models that combine algorithmic models with stochastic exposure simulators to estimate human exposure to toxins (Gelfand and Sahu, 2010). Surprisingly, propagating uncertainty in this way is exceedingly rare in ecology. A notable exception is the work of McInerny and Purves (2011), which provides an interesting application of a hierarchical species distribution model to account for both environmental uncertainty (measurement error) and sub-pixel variability. They found that adding a latent variable for the 'true' (but unknown) environment actually reduced regression dilution by allowing sub-pixel environmental variability and enabled improved predictions of species distributions. Furthermore, multi-species models with common latent environmental variables dramatically improved model performance by increasing the constraints on both latent variables and species parameters. Climate data that include careful quantification of uncertainties, such as those produced in this study, should facilitate the development of a richer and more robust predictive modeling in ecology and biogeography.

4.2 Potential Enhancements

The methodology presented here could be further enhanced in several ways. For example, due to computational limitations we were limited to interpolating the anomalies at $^1/_4$ degree resolution even over this relatively small region. Use of a "predictive process" spatial model (Banerjee et al., 2008) to decrease the size of the spatial covariance matrix would facilitate increasing the size of the region (and number of stations) while still accounting for spatial autocorrelation (Chakraborty et al., 2011). Additionally, our method ignores the uncertainty present in the underlying interpolated long-term climate surfaces. This was unavoidable because no uncertainty estimates were available (Schulze, 2007) which is usually the case for long-term climate summaries. Future analyses could rectify this situation by first generating high resolution climate surfaces (with uncertainty estimates) prior to interpolating daily anomalies. It would also be possible to incorporate other sources of information at either the climatic or daily anomaly stage, including topographic variables, distance to nearest coast, land cover type, satellite observations of temperature or clouds (*e.g.* Alvarez-Villa et al., 2011; Hart et al., 2009) or results from a coarse-grained reanalysis of global meteorological data (*e.g* Compo et al., 2011).

5 Conclusion

Various methods have been employed to understand how environmental change will impact biodiversity, including models of species distributions (e.g. Franklin et al., 2012) and demographic processes (e.g. Jenouvrier et al., 2012). Typically, practitioners 1) fit a model using historical explanatory data, which often includes interpolated climate data and/or remotely sensed products and then 2) use that model to project into the future using climate model output. In other words, models constructed to forecast biodiversity often use 'output' from other models as 'input' data. However, in most cases the uncertainties presented in the results are derived only from the biological model and ignore uncertainties in the source datasets. Statistically, this is a reasonable approach with the important caveat that the results are conditional on the input datasets. But for decision-making purposes, it is important that the uncertainties represent the overall confidence in the forecast. The IPCC, for example, has standardized how uncertainties should be handled and described throughout their publications (Mastrandrea et al., 2010) and other disciplines, such as hydrology, have taken this problem seriously (e.g. Liu and Gupta, 2007). Thus ecologists are faced with the important challenge of propagating uncertainties inherent in source datasets through new models to the final results. In this study we introduced a method to generate continuous surfaces of ecologically relevant climate metrics that include estimates of uncertainty introduced by the interpolating from station values. We also presented a simple example of how this sort of data could be used in a hierarchical distribution model to further propagate the uncertainty through to ecological predictions. The methodology presented here could have wide application for ecological models capable of incorporating and propagating data uncertainty through to the model output and results. This will likely lead to projections with wider prediction intervals that we can be more confident in.

References

Ahmed, K., Wang, G., Silander Jr, J., Wilson, A. M., and Allen, J. M. 2013. Bias correctionand downscaling of climate model outputs for climate change impact assessmentsin the U.S. northeast. *Global and Planetary Change*, 100(2013):320—332.

Alvarez-Villa, O. D., Velez, J. I., and Poveda, G. 2011. Improved long-term mean annual rainfall fields for colombia. *International Journal of Climatology*, 31(14):21942212.

Apaydin, H., Sonmez, F. K., and Yildirim, Y. E. 2004. Spatial interpolation techniques for climate data in the GAP region in turkey. *Climate Research*, 28(1):3140.

Banerjee, S., Gelfand, A. E., Finley, A. O., and Sang, H. 2008. Gaussian predictive process models for large spatial data sets. *Journal of the Royal Statistical Society: Series B (Statistical Methodology)*, 70(4):825–848.

Beaumont, L., Hughes, L., and Pitman, A. 2008. Why is the choice of future climate scenarios for species distribution modelling important? *Ecology Letters*, 11(11):11351146.

Bhner, J. 2005. *Advancements and new approaches in climate spatial prediction and environmental modelling.* Arbeitsberichte des Geographischen Instituts der HU, Berlin, Germany.

Chakraborty, A., Gelfand, A. E., Wilson, A. M., Latimer, A. M., and Silander, J. 2010. Modeling large scale species abundance with latent spatial processes. *The Annals of Applied Statistics*, 4(3):1403—1429.

Chakraborty, A., Gelfand, A. E., Wilson, A. M., Latimer, A. M., and Silander, J. A. 2011. Point pattern modeling for degraded presence-only data over large regions. *Journal of the Royal Statistical Society. Series C (Applications)*, 60(5):757—776.

Christensen, J., Hewitson, B., Busuioc, A., Chen, A., Gao, X., Held, R., Jones, R., Kolli, R., Kwon, W., and Laprise, R. 2007. Chapter 11: Regional climate projections. In *Regional climate projections, Climate Change, 2007: The Physical Science Basis. Contribution of Working group I to the Fourth Assessment Report of the Intergovernmental Panel on Climate Change*. University Press, Cambridge.

Clark, J. S. 2003. Uncertainty and variability in demography and population growth: a hierarchical approach. *Ecology*, 84(6):13701381.

Clark, J. S. 2004. Why environmental scientists are becoming bayesians. *Ecology letters*, 8(1):214.

Clark, J. S., Agarwal, P., Bell, D. M., Flikkema, P. G., Gelfand, A., Nguyen, X., Ward, E., and Yang, J. 2011. Inferential ecosystem models, from network data to prediction. *Ecological Applications*, 21(5):1523–1536.

Clark, J. S., Carpenter, S. R., Barber, M., Collins, S., Dobson, A., Foley, J. A., Lodge, D. M., Pascual, M., Jr., R. P., Pizer, W., Pringle, C., Reid, W. V., Rose, K. A., Sala, O., Schlesinger, W. H., Wall, D. H., and Wear, D. 2001. Ecological forecasts: An emerging imperative. *Science*, 293(5530):657 –660.

Clark, J. S. and Gelfand, A. E. 2006. A future for models and data in environmental science. *Trends in Ecology & Evolution*, 21(7):375—380.

Colchero, F., Medellin, R. A., Clark, J. S., Lee, R., and Katul, G. G. 2009. Predicting population survival under future climate change: density dependence, drought and extraction in an insular bighorn sheep. *Journal of Animal Ecology*, 78(3):666673.

Collins, M., Booth, B. B., Harris, G. R., Murphy, J. M., Sexton, D. M., and Webb, M. J. 2006a. Towards quantifying uncertainty in transient climate change. *Climate Dynamics*, 27(2):127147.

Collins, S., Bettencourt, L., Hagberg, A., Brown, R., Moore, D., Bonito, G., Delin, K., Jackson, S., Johnson, D., Burleigh, S., et al. 2006b. New opportunities in ecological sensing using wireless sensor networks. *Frontiers in Ecology and the Environment*, 4(8):402407.

Compo, G., Whitaker, J., Sardeshmukh, P., Matsui, N., Allan, R., Yin, X., Gleason, B., Vose, R., Rutledge, G., Bessemoulin, P., et al. 2011. The twentieth century reanalysis project. *Quarterly Journal of the Royal Meteorological Society*, 137(654):128.

Cooley, D., Nychka, D., and Naveau, P. 2007. Bayesian spatial modeling of extreme precipitation return levels. *Journal of the American Statistical Association*, 102:824–840.

Cressie, N., Calder, C. A., Clark, J. S., Hoef, J. M. V., and Wikle, C. K. 2009. Accounting for uncertainty in ecological analysis: the strengths and limitations of hierarchical statistical modeling. *Ecological Applications*, 19(3):553570.

Cressman, G. P. 1959. An operational objective analysis system. *Monthly Weather Review*, 87(10):367–374.

Daly, C. 2006. Guidelines for assessing the suitability of spatial climate data sets. *International Journal of Climatology*, 26(6):707721.

Diggle, P. J. and Ribeiro, P. J. 2007. *Model-based geostatistics*, volume 846. Springer New York.

Diggle, P. J. and Ribeiro Jr, P. J. 2001. geo{R}: a package for geostatistical analysis. *R-News*, 1(2):14–18.

Diggle, P. J. and Ribeiro Jr, P. J. 2002. Bayesian inference in gaussian model-based geostatistics. *Geographical and Environmental Modelling*, 6(2):129146.

Elith, J., Phillips, S., Hastie, T., Dudk, M., Chee, Y., and Yates, C. 2011. A statistical explanation of MaxEnt for ecologists. *Diversity and Distributions*.

Fasbender, D. and Ouarda, T. B. 2010. Spatial bayesian model for statistical downscaling of AOGCM to minimum and maximum daily temperatures. *Journal of Climate*, 23(19):52225242.

Feddema, J. 2005. A revised thornthwaite-type global climate classification. *Physical Geography*, 26(6):442–466.

Fischer, A. M., Weigel, A. P., Buser, C. M., Knutti, R., Kuensch, H. R., Liniger, M. A., Schaer, C., and Appenzeller, C. 2012. Climate change projections for switzerland based on a bayesian multi-model approach. *International Journal of Climatology*, 32(15):2348–2371. WOS:000312033900008.

Franklin, J., Davis, F. W., Ikegami, M., Syphard, A. D., Flint, L. E., Flint, A. L., and Hannah, L. 2012. Modeling plant species distributions under future climates: how fine scale do climate projections need to be? *Global Change Biology*, pages 1—11.

Gelfand, A. and Sahu, S. 2010. Combining monitoring data and computer model output in assessing environmental exposure. In *The Oxford Handbook of Applied Bayesian Analysis*, page 896. Oxford University Press, USA.

Goldblatt, P. 1997. Floristic diversity in the cape flora of south africa. *Biodiversity and Conservation*, 6(3):359377.

Guan, B. T., Hsu, H. W., Wey, T. H., and Tsao, L. S. 2009. Modeling monthly mean temperatures for the mountain regions of taiwan by generalized additive models. *Agricultural and Forest Meteorology*, 149(2):281290.

Gutschick, V. P. and BassiriRad, H. 2003. Extreme events as shaping physiology, ecology, and evolution of plants: toward a unified definition and evaluation of their consequences. *New Phytologist*, 160(1):21—42.

Hart, Q. J., Brugnach, M., Temesgen, B., Rueda, C., Ustin, S. L., and Frame, K. 2009. Daily reference evapotranspiration for california using satellite imagery and weather station measurement interpolation. *Civil Engineering and Environmental Systems*, 26(1):1933.

Haylock, M. R., Hofstra, N., Klein Tank, A. M. G., Klok, E. J., Jones, P. D., and New, M. 2008. A european daily high-resolution gridded dataset of surface temperature and precipitation. *J. Geophys. Res*, 113:D20119.

Hijmans, R. J., Cameron, S. E., Parra, J. L., Jones, P. G., Jarvis, A., and Others 2005. Very high resolution interpolated climate surfaces for global land areas. *International Journal of Climatology*, 25(15):1965—1978.

Hunter, R. D. and Meentemeyer, R. K. 2005. Climatologically aided mapping of daily precipitation and temperature. *Journal of Applied Meteorology*, 44(10):1501—1510.

Iizumi, T., Nishimori, M., Yokozawa, M., Kotera, A., and Khang, N. D. 2012. Statistical downscaling with bayesian inference: Estimating global solar radiation from reanalysis and limited observed data. *International Journal of Climatology*, 32(3):464–480. WOS:000300934000013.

Jackson, S. T., Betancourt, J. L., Booth, R. K., and Gray, S. T. 2009. Ecology and the ratchet of events: Climate variability, niche dimensions, and species distributions. *Proceedings of the National Academy of Sciences*, 106:19685–19692.

Jenouvrier, S., Holland, M., Stroeve, J., Barbraud, C., Weimerskirch, H., Serreze, M., and Caswell, H. 2012. Effects of climate change on an emperor penguin population: analysis of coupled demographic and climate models. *Global Change Biology*.

Johansson, M. A. and Glass, G. E. 2008. High-resolution spatiotemporal weather models for climate studies. *International journal of health geographics*, 7(1):52.

Johns, T. C., Carnell, R. E., Crossley, J. F., Gregory, J. M., Mitchell, J. F. B., Senior, C. A., Tett, S. F. B., and Wood, R. A. 1997. The second hadley centre coupled ocean-atmosphere GCM: model description, spinup and validation. *Climate Dynamics*, 13(2):103–134.

Keeley, J. and Bond, W. 1997. Convergent seed germination in south african fynbos and californian chaparral. *Plant Ecology*, 133(2):153167.

Kimball, S., Gremer, J. R., Angert, A. L., Huxman, T. E., and Venable, D. L. 2012. Fitness and physiology in a variable environment. *Oecologia*, page 111.

Latimer, A. M., Silander, J. A., and Cowling, R. M. 2005. Neutral ecological theory reveals isolation and rapid speciation in a biodiversity hot spot. *Science*, 309(5741):17221725.

Lawler, J. J., Shafer, S. L., White, D., Kareiva, P., Maurer, E. P., Blaustein, A. R., and Bartlein, P. J. 2009. Projected climate-induced faunal change in the western hemisphere. *Ecology*, 90(3):588–597.

Liu, Y. and Gupta, H. V. 2007. Uncertainty in hydrologic modeling: Toward an integrated data assimilation framework. *Water Resources Research*, 43(7):n/an/a.

Luo, Y., Ogle, K., Tucker, C., Fei, S., Gao, C., LaDeau, S., Clark, J. S., and Schimel, D. S. 2011. Ecological forecasting and data assimilation in a data-rich era. *Ecological Applications*, 21(5):14291442.

Mastrandrea, M. D., Field, C. B., Stocker, T. F., Edenhofer, O., Ebi, K. L., Frame, D. J., Held, H., Kriegler, E., Mach, K. J., Matschoss, P. R., Plattner, G.-K., and Yohe, G. 2010. Guidance note for lead authors of the IPCC fifth assessment report on consistent treatment of uncertainties. IPCC cross-working group meeting on consistent treatment of uncertainties, Intergovernmental Panel on Climate Change, Jasper Ridge, CA, USA.

McInerny, G. J. and Purves, D. W. 2011. Fine-scale environmental variation in species distribution modelling: regression dilution, latent variables and neighbourly advice. *Methods in Ecology and Evolution*, 2(3):248257.

Meyen, F. J. F. 1846. *Outlines of the Geography of Plants: With Particular Enquiries Concerning the Native Country, the Culture, and the Uses of the Principal Cultivated Plants on Which the Prosperity of Nations Is Based*. The Ray Society. Printed for the Ray Society, London.

Midgley, J. J. 1988. Mortality of cape proteaceae seedlings during their first summer. *South African Forestry Journal*, 145:9–12.

Mueller, R. and Schulzweida, U. 2013. Climate data operators.

Muraoka, H. and Koizumi, H. 2009. Satellite ecology (SATECO)linking ecology, remote sensing and micrometeorology, from plot to regional scale, for the study of ecosystem structure and function. *Journal of plant research*, 122(1):320.

{National Center for Atmospheric Research} 2011. NCAR command language. http://www.ncl.ucar.edu/.

Newlands, N. K., Davidson, A., Howard, A., and Hill, H. 2011. Validation and intercomparison of three methodologies for interpolating daily precipitation and temperature across canada. *Environmetrics*, 22(2):205–223.

Pearson, R., Raxworthy, C., Nakamura, M., and Peterson, A. 2007. Predicting species distributions from small numbers of occurrence records: a test case using cryptic geckos in madagascar. *Journal of Biogeography (J. Biogeogr.)*, 34:102117.

Peterson, A. and Nakazawa, Y. 2008. Environmental data sets matter in ecological niche modelling: an example with solenopsis invicta and solenopsis richteri. *Global Ecology and Biogeography*, 17(1):135.

Raes, N., Roos, M. C., Slik, J. W. F., Van Loon, E. E., and Steege, H. T. 2009. Botanical richness and endemicity patterns of borneo derived from species distribution models. *Ecography*, 32(1):180192.

{R Development Core Team} 2011. R: A language and environment for statistical computing.

Ribeiro Jr, P. J. and Diggle, P. J. 2009. Bayesian inference in gaussian model-based geostatistics. Technical Report ST-99-08, Department of Mathematics and Statistics,Lancaster University, LA1 4YF Lancaster-UK.

Riccio, A. 2005. A bayesian approach for the spatiotemporal interpolation of environmental data. *Monthly weather review*, 133(2):430440.

Richardson, A. D., Bailey, A. S., Denny, E. G., Martin, C. W., and O'keefe, J. 2006. Phenology of a northern hardwood forest canopy. *Global Change Biology*, 12(7):11741188.

Roubicek, A., VanDerWal, J., Beaumont, L., Pitman, A., Wilson, P., and Hughes, L. 2010. Does the choice of climate baseline matter in ecological niche modelling? *Ecological Modelling*, 221(19):22802286.

Ruggieri, E. 2013. A bayesian approach to detecting change points in climatic records. *International Journal of Climatology*, 33(2):520–528. CCC:000313753900020.

Sang, H. and Gelfand, A. E. 2009. Hierarchical modeling for extreme values observed over space and time. *Environmental and Ecological Statistics*, 16(3):407–426.

Schulze, R. E. 2007. The south african atlas of agrohydrology and climatology. Technical Report WRC Report 1489/1/06, Water Research Commission, Pretoria, South Africa.

Soria-Auza, R., Kessler, M., Bach, K., Barajas-Barbosa, P., Lehnert, M., Herzog, S., and Bhner, J. 2010. Impact of the quality of climate models for modelling species occurrences in countries with poor climatic documentation: a case study from bolivia. *Ecological Modelling*, 221(8):12211229.

Stahl, K., Moore, R. D., Floyer, J. A., Asplin, M. G., and McKendry, I. G. 2006. Comparison of approaches for spatial interpolation of daily air temperature in a large region with complex topography and highly variable station density. *Agricultural and Forest Meteorology*, 139(3-4):224236.

Tait, A., Henderson, R., Turner, R., and Zheng, X. 2006. Thin plate smoothing spline interpolation of daily rainfall for new zealand using a climatological rainfall surface. *International Journal of Climatology*, 26(14):2097–2115.

Tebaldi, C. and Knutti, R. 2007. The use of the multi-model ensemble in probabilistic climate projections. *Philosophical Transactions of the Royal Society A: Mathematical, Physical and Engineering Sciences*, 365(1857):20532075.

Trnka, M., Olesen, J. E., Kersebaum, K. C., Skjelvg, A. O., Eitzinger, J., Seguin, B., Peltonen-Sainio, P., Rtter, R., Iglesias, A., Orlandini, S., Dubrovsk, M., Hlavinka, P., Balek, J., Eckersten, H., Cloppet, E., Calanca, P., Gobin, A., Vueti, V., Nejedlik, P., Kumar, S., Lalic, B., Mestre, A., Rossi, F., Kozyra, J., Alexandrov, V., Semerdov, D., and alud, Z. 2011. Agroclimatic conditions in europe under climate change. *Global Change Biology*, 17(7):22982318.

Ward, D. 2007. Modelling the potential geographic distribution of invasive ant species in new zealand. *Biological Invasions*, 9(6):723735.

Wiens, J., Stralberg, D., Jongsomjit, D., Howell, C., and Snyder, M. 2009. Niches, models, and climate change: assessing the assumptions and uncertainties. *Proceedings of the National Academy of Sciences*, 106(Supplement 2):19729.

Williams, J., Seo, C., Thorne, J., Nelson, J., Erwin, S., OBrien, J., and Schwartz, M. 2009. Using species distribution models to predict new occurrences for rare plants. *Diversity and Distributions*, 15(4):565576.

Williams, C. N., J., Menne, M., Vose, R., and Easterling, D. 2006. United states historical climatology network daily temperature, precipitation, and snow data. Technical Report ORNL/CDIAC-118, NDP-070, Carbon Dioxide Information Analysis Center, Oak Ridge National Laboratory, Oak Ridge, Tennessee.

Willmott, C. and Robeson, S. 1995. Climatologically aided interpolation (CAI) of terrestrial air temperature. *International Journal of Climatology*, 15(2):221229.

Wilson, A. M., Latimer, A. M., Silander, J. A., Gelfand, A. E., and de Klerk, H. 2010. A hierarchical bayesian model of wildfire in a mediterranean biodiversity hotspot: Implications of weather variability and global circulation. *Ecological Modelling*, 221(1):106—112.

Zender, C. 2008. Analysis of self-describing gridded geoscience data with netCDF operators (NCO). *Environmental Modelling & Software*, 23(10-11):13381342.